



STATE RESEARCH CENTER OF RUSSIA  
INSTITUTE FOR HIGH ENERGY PHYSICS

FERMI LAB

OCT 22 1997

IHEP 97-13

G.I.Britvich\*, F.Galeazzi<sup>+</sup>, S.V.Golovkin\* G.Martellotti<sup>+</sup>,  
A.M.Medvedkov\*, G.Penso<sup>+</sup>, A.S.Solovjev\*\*, V.G.Vasil'chenko\*



**LUMINESCENT PROPERTIES  
OF FROZEN SCINTILLATORS**

\*Institute for High Energy Physics, 142284, Protvino, Russian Federation

<sup>+</sup>INFN, Rome, Italy

\*\*Joint Institute for Nuclear Research, 141980, Dubna, Russian Federation

Protvino 1997

### Abstract

Britvich G.I. et al. Luminescent Properties of Frozen Scintillators: IHEP Preprint 97-13. – Protvino, 1997. – p. 10, figs. 11, tables 3, refs.: 10.

Temperature dependencies of the light outputs of liquid and frozen scintillators have been investigated. Frozen in vacuum to a temperature of about  $-120^{\circ}\text{C}$  green emitting light scintillators based on 1-methylnaphthalene solvent enhanced their light outputs up to 2.2-3.3 times relative to the levels in their liquid states at room temperature in air. For scintillators frozen in vacuum their light outputs reached levels of 92-144 % in comparison with an anthracene under high energy  $\beta$ -particles excitation. In the processes of cooling down to a temperature of about  $-120^{\circ}\text{C}$  and then heating up to  $20^{\circ}\text{C}$  all the tested scintillators in some temperature intervals revealed the effects of thermal hysteresis of their light outputs. Signals duration of frozen scintillators in air increased in comparison with those at room temperature. The light outputs of these tested scintillators are sensitive to the density of ionization.

### Аннотация

Бритвич Г.И. и др. Люминесцентные свойства замороженных сцинтилляторов: Препринт ИФВЭ 97-13. – Протвино, 1997. – 10 с., 11 рис., 3 табл., библиогр.: 10.

Приведены результаты исследований температурных зависимостей световых выходов жидких и замороженных сцинтилляторов. Замороженные в вакууме при температуре около  $-120^{\circ}\text{C}$  сцинтилляторы на основе 1-метилнафталина, излучающие свет в зеленой области спектра, показали увеличение своего световыхода в 2.2-3.3 раза по сравнению с их уровнями при комнатной температуре на воздухе. Световыход замороженных в вакууме сцинтилляторов достиг значений 92-144% от кристалла антрацена при возбуждении  $\beta$ -частицами высоких энергий. В процессе охлаждения до температуры  $-120^{\circ}\text{C}$  и затем нагревания до  $+20^{\circ}\text{C}$  все исследованные сцинтилляторы показали эффект температурного гистерезиса своего световыхода. Длительность сигналов от замороженных на воздухе сцинтилляторов несколько удлинилась по сравнению с их длительностями при комнатной температуре. Световыход исследованных сцинтилляторов чувствителен к плотности ионизации.

## Introduction

The main advantages of recently found green emitting light liquid scintillators (LSs) at a temperature  $T=20^{\circ}\text{C}$  in air [1-6] are high levels of the light outputs which are up to 1.34-1.52 times higher in comparison with a standard polystyrene scintillator containing 1.5% pTP + 0.01% POPOP, relatively short decay time constants of about 6.2-7.6 ns [3,5,6] and high levels of radiation hardness  $>100$  Mrad [7]. Abbreviations and known to us chemical formulae of the used solvents, dopants, their peak emission wavelengths  $\lambda_{em}$  in 1MN and freezing points of solvents  $T_f$  are listed in Appendix. We also measured for the scintillation dopants  $\lambda_{em}$  in IPN. It was found that they are close to the data presented in Appendix.

Some improvements of LSs light outputs in vacuum and neutral gas atmospheres are presented elsewhere [8]. Here we continue our investigation of other possibilities to increase scintillators light outputs. That is important for many applications especially for different types of particle detectors and calorimeters based on organic scintillators in high energy physics, for ionizing radiation detection in nuclear physics, etc.

This work is devoted to the investigation of luminescent properties of our promising scintillators at low temperatures.

### 1. Experimental technique

Our LSs were cooled down in a glass ampoule. Below their  $T_f$  the bulk of frozen scintillators based on 1MN was semitransparent. Most of the frozen scintillators based on 1PN and IPN were transparent. Our preliminary investigation showed that the optical properties of frozen scintillators were greatly dependent on the samples thickness, their rate of cooling down, especially at the point of state transition  $T_f$ , etc. Because of this we had to use relatively thin layers of frozen scintillators in our light output measurements, i.e.  $\sim 0.1$  cm, in order to minimize the effect of light losing due to the self-absorption.

At first we determined the light output  $I$  at  $T=20^{\circ}\text{C}$  in air and vacuum of a scintillator based on IPN containing R6 dopant (IPN + R6) with a concentration of about 3g/l.

We measured relative positions of their total absorption peaks for  $\sim 976$  keV conversion electrons from a  $^{207}\text{Bi}$  radioactive source in this 0.5 cm thick scintillator. The source and samples were fixed upon the entrance window of a photoreceiver, a photomultiplier (PM) FEU-84-3. The PM quantum efficiency  $Y$  is presented in Fig. 1. The integration time in the pulse height analyzing channel was about 400 ns. Experimental results of the pulse height measurements for  $\varnothing 1.6 \times 0.5\text{cm}^3$  scintillator samples in its liquid state are presented in Fig.2. The light output of IPN + R6 at  $T=20^\circ\text{C}$  in air and vacuum reached 36.5 % and 46 %, respectively, in comparison with a crystal anthracene having a comparative size.

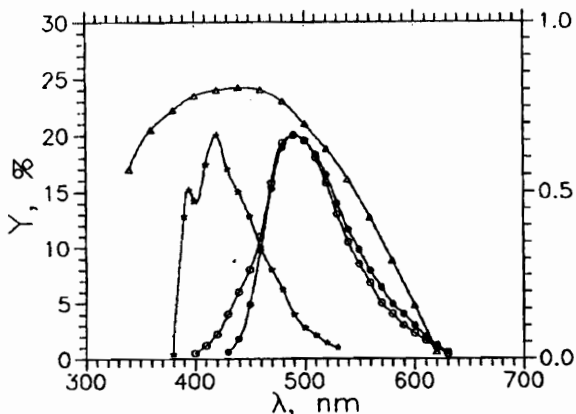


Fig. 1. Quantum efficiency  $Y$  of our PM ( $\Delta$ ) and luminescent spectra  $L$  of our PS scintillator ( $\star$ ), 1MN + R6 in air at  $T=20^\circ\text{C}$  ( $\bullet$ ) and 1MN + R6 in air at  $T=-120^\circ\text{C}$  ( $\circ$ ) for the excitation at 365 nm.

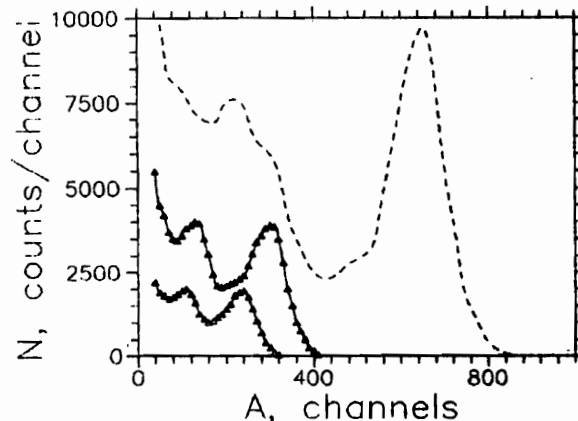


Fig. 2. Pulse height spectra of scintillation signals from  $^{207}\text{Bi}$  in IPN + R6 (solid lines) and anthracene (dashed line).  $\Delta$  - at  $20^\circ\text{C}$  in air;  $\blacktriangle$  - at  $20^\circ\text{C}$  in vacuum.

On the one hand, this technique of total absorption peaks measurements required a lot of time for the accumulation of necessary statistics during which it was difficult for us to keep scintillators temperature relatively constant in our setup. On the other hand, the required scintillator thickness ( $\geq 0.5$  cm) for such measurements did not allow us to get good optical properties in all the frozen scintillator samples. Because of that we used this technique mainly for calibration purposes.

For all comparative tests the light output of our scintillators was measured by exciting the samples ( $\varnothing 1.6 \times 0.1\text{cm}^3$ ) with a  $^{90}\text{Sr}$  radioactive  $\beta$ -source. The source and samples were fixed upon the entrance window of the PM. There was no optical contact between the scintillators and PM entrance window because we had not found any grease, which could provide it at low temperatures down to  $T=-120^\circ\text{C}$ . The PM photocurrent was measured. The light output  $I$  of our scintillators was also determined in comparison with a crystal anthracene without taking into account the PM quantum efficiency. As appeared, the results of this technique of measurements are in a good agreement with the results of total absorption peaks measurements and this will be shown below.

The light output of our crystal anthracene at  $T=20^\circ\text{C}$  was set equal to 100%. Note that in some cases the light outputs of our scintillators were also measured in comparison

with a standard PS scintillator containing 1.5% + 0.01% POPOP having the light output of about 25% in comparison with anthracene [8]. The luminescent spectra L of POPOP and R6 are presented in Fig. 1. As is clear from Fig. 1 the PM quantum efficiency plateau is relatively broad and overlaps the maxima of emission spectra of our blue (PS and anthracene with  $\lambda_{em}=447$  nm) and green scintillators. The luminescent properties of our other scintillating dopants were presented elsewhere [6].

The instrumentation error of the light output was determined on the base of repeated measurements and was about  $\pm 2\%$  with a possible systematic error of about  $\pm 8\%$ . The concentration of scintillating dopants in our scintillators was about 3 g/l. Other levels of the dopant concentration will be especially mentioned hereafter.

The scintillator samples were initially cooled down from  $T=20^\circ\text{C}$  to  $T=-120^\circ\text{C}$  and then heated up from  $T=-120^\circ\text{C}$  to  $T=20^\circ\text{C}$ . Preliminary investigations showed that the light outputs of frozen scintillators based on 1MN were up to  $\pm 10\%$  dependent on the rate of the samples temperature changing, when it was  $|\Delta T| \geq 2^\circ\text{C}/\text{min}$ . That is the reason why the mean rate of the scintillator samples temperature changing in our measurements was chosen to be about  $\Delta T \simeq \pm 1^\circ\text{C}/\text{min}$ .

## 2. Experimental results

### 2.1. Influence of low temperature on scintillators light output

We investigated the light output temperature dependencies for some green emitting light scintillators based on liquid solvents at  $T=20^\circ\text{C}$ , i.e. 1MN, IPN and 1PN, and our promising scintillating dopants, i.e. R6, R39, R45 and 3M-15 [6].

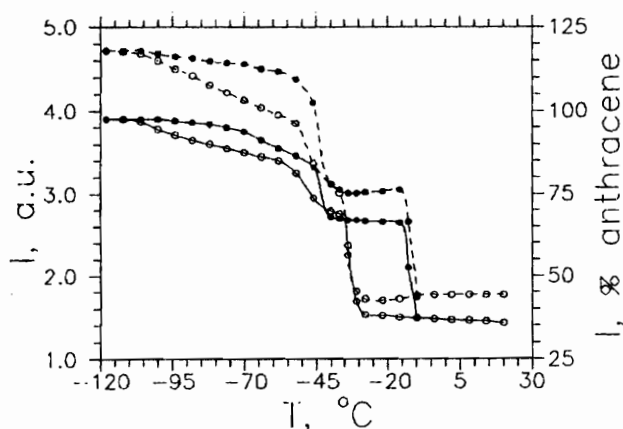


Fig. 3. Light output of 1MN + R45 versus temperature.  $\circ$  – for cooling down with  $\Delta T=-1^\circ\text{C}/\text{min}$  and  $\bullet$  – for heating up with  $\Delta T=1^\circ\text{C}/\text{min}$ ; solid lines – in air and dashed lines – in vacuum. Light output of our PS scintillator was taken as 1.

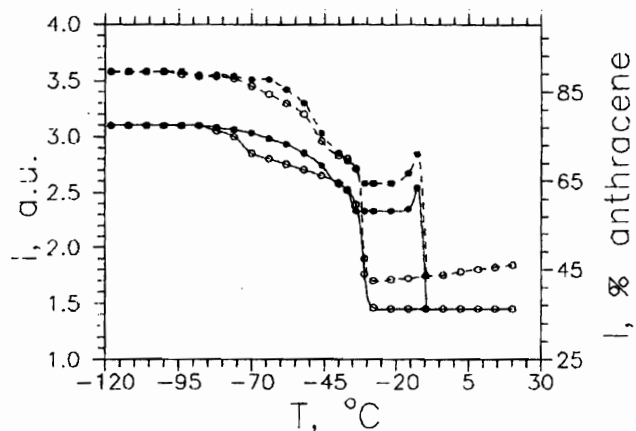


Fig. 4. Light output of 1MN + R6 versus temperature.  $\circ$  – for cooling down and  $\bullet$  – for heating up; solid lines – in air and dashed lines – in vacuum. Light output of our PS scintillator was taken as 1.

Some results of this investigation are presented in Figs. 3-8. All the scintillators frozen in air down to  $T=-120^{\circ}\text{C}$ , i.e. in their solid states, showed significant light output  $I_{sa}$  enhancements in comparison with those levels at  $T=20^{\circ}\text{C}$  in air  $I_{la}$ , i.e. in their liquid states. They practically reached their maximum levels at  $T=-120^{\circ}\text{C}$ . Experimental results for some scintillators based on 1MN are presented in Figs. 3-4. Among scintillators frozen in vacuum the maximum light output  $I_{sv}=118\%$  in comparison with the anthracene showed 1MN + R45 (Fig. 3). This light output level is about 3.3 times higher relative to that ( $I_{la}=35.8\%$ ) at  $T=20^{\circ}\text{C}$  in air. Note these results were acquired without taking into account the quantum efficiency of our PM presented in Fig. 1.

The light output of IPN + R6 at  $T=20^{\circ}\text{C}$  in air and vacuum (Fig. 5) reached  $I_{la}=36.3\%$  and  $I_{lv}=47.8\%$ , respectively, in comparison with the anthracene under the high energy  $\beta$ -particles excitation. Note that these scintillator light outputs coincided well within the accuracy of such measurements with the light output values obtained in the relative positions of total absorption peaks measurements (Fig. 2). Some experimental results on 1PN + R6 light output temperature dependencies are presented in Fig. 6. Our main experimental results for our best scintillators are summarized in Table 1.

**Table 1.** Luminescent properties of our best scintillators under high energy  $\beta$ -particles excitation.

N	Solvent	Dopant	$I_{la},\%$	$I_{la}^y,\%$	$I_{lv},\%$	$I_{lv}^y,\%$	$I_{sa},\%$	$I_{sa}^y,\%$	$I_{sv},\%$	$I_{sv}^y,\%$
1	1MN	R6	36.3	46.8	46.0	59.2	67.5	83.7	89.5	109.
2		R45	35.8	47.3	44.3	58.6	85.0	110.	118.	144.
3		R39	38.0	47.9	50.3	63.2	67.3	80.8	99.3	120.
4		3M-15	33.5	44.2	41.5	54.9	89.8	116.	101.	123.
5	IPN	R6	36.3	46.7	47.8	61.8	82.0	101.	88.3	109.
6		R45	33.8	44.6	42.8	56.6	71.3	85.6	77.5	94.6
7		R39	36.8	46.4	47.3	59.5	60.0	73.8	77.0	92.4
8		3M-15	37.5	49.5	45.5	60.0	78.8	94.6	87.0	106.

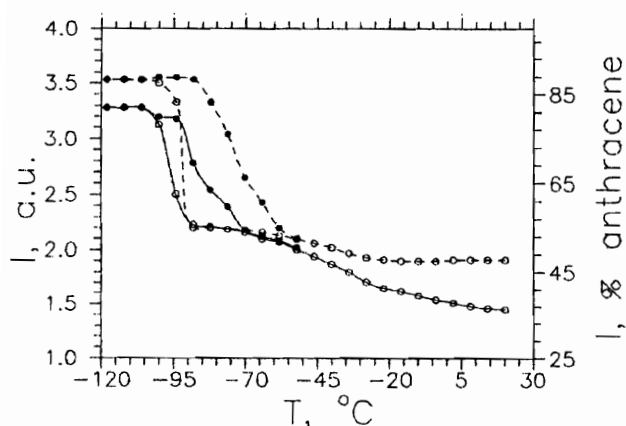


**Fig. 5.** Light output of IPN + R6 versus temperature.  $\circ$  – for cooling down and  $\bullet$  – for heating up; solid lines – in air and dashed lines – in vacuum. Light output of our PS scintillator was taken as 1.

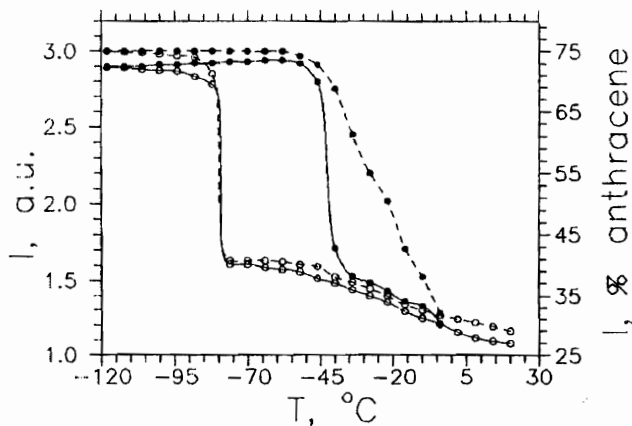


**Fig. 6.** Light output of 1PN + R6 versus temperature.  $\circ$  – for cooling down and  $\bullet$  – for heating up; solid lines – in air and dashed lines – in vacuum. Light output of our PS scintillator was taken as 1.

For our best scintillators frozen down to  $T=-120^{\circ}\text{C}$  we measured their luminescent spectra. Some results of these measurements are presented in Fig. 1. Taking into account the PM quantum efficiency, the emission spectra of the LSs [7] and the scintillators frozen down to  $T=-120^{\circ}\text{C}$  in air and vacuum, and experimental data from Table 1, we can estimate the intrinsic light outputs of the LSs in air  $I_{la}^y$  and in vacuum  $I_{lv}^y$  at  $T=20^{\circ}\text{C}$  [7] and for the scintillators frozen down to  $T=-120^{\circ}\text{C}$  in air  $I_{sa}^y$  and in vacuum  $I_{sv}^y$ . Note that the error of  $I_{sa}^y$  and  $I_{sv}^y$  estimations was about  $\pm 15\%$ . As is clear from Table 1 their maximum light outputs in vacuum have reached the levels of 92-144 % in comparison with the anthracene. Experimental data for other less efficient scintillators are summarized in Table 2.

**Table 2.** Luminescent properties of other scintillators under high energy  $\beta$ -particles excitation.

N	Solvent	Dopant	$I_{la},\%$	$I_{lv},\%$	$I_{sa},\%$	$I_{sv},\%$
1	IPN	R6	27.0	29.0	72.3	75.0
2		R45	20.0	22.0	56.3	57.3
3		R39	25.3	28.0	53.0	55.3
4		3M-15	23.5	26.3	50.3	54.3

The frozen pure solvents also showed high light output enhancements in comparison with those levels at  $T=20^{\circ}\text{C}$  reaching their maximum levels at  $T=-120^{\circ}\text{C}$ . Some results of our measurements for pure 1MN and IPN are presented in Fig. 7-8. As is clear from Fig. 7 frozen down to  $T=-120^{\circ}\text{C}$  in vacuum pure 1MN showed the light output comparative with that of the frozen 1MN + R45. Obviously, that such high levels of frozen scintillators light outputs were due to enhanced levels of the light output of their frozen solvents.

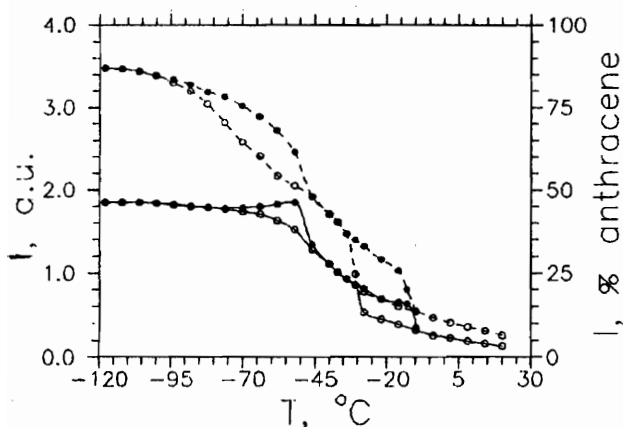


**Fig. 7.** Light output of pure 1MN versus temperature.  $\circ$  – for cooling down and  $\bullet$  – for heating up; solid lines – in air and dashed lines – in vacuum. Light output of our PS scintillator was taken as 1.

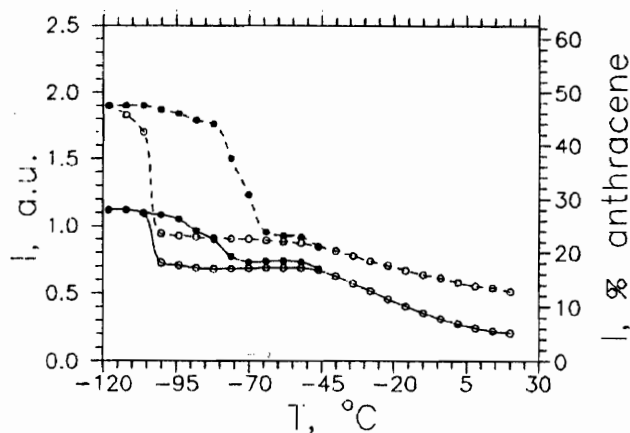


**Fig. 8.** Light output of pure IPN versus temperature.  $\circ$  – for cooling down and  $\bullet$  – for heating up; solid lines – in air and dashed lines – in vacuum. Light output of our PS scintillator was taken as 1.

Fig. 9 presents frozen at  $T=-120^{\circ}\text{C}$  1MN + R6 light outputs in vacuum and air as a function of R6 concentration. Frozen scintillators showed their maximum light outputs at lower concentration levels in comparison with an optimal concentration  $c=3\text{g/l}$  for the scintillators light outputs at  $T=20^{\circ}\text{C}$  in air [6].

We also determined the light outputs of 1MN + R45 frozen in air and vacuum by measuring relative positions of their total absorption peaks of 60 keV  $\gamma$ -quanta from a  $^{241}\text{Am}$  radioactive source in thin ( $\sim 0.1$  cm) layers of the scintillator. Some experimental results of the pulse height measurements for the scintillator in liquid and solid (at  $T=-120^{\circ}\text{C}$ ) states are presented in Fig. 10. From the data presented in Fig. 10 one can see that the luminescent efficiency of 1MN + R45 frozen in vacuum down to  $T=-120^{\circ}\text{C}$  reached a level of about 60 % in comparison with the anthracene under such low energy  $\gamma$ -quanta excitation. Note that absolute values of all the scintillator light outputs presented in Fig. 10 and measured under low energy  $\gamma$ -quanta excitation are about 2 times lower against those under high energy  $\beta$ -particles excitation presented in Fig. 3 for the same scintillator. Obviously, that the light outputs of our scintillators both in the liquid and solid states are sensitive to the density of ionization. Due to this effect we had clear pictures of interaction events near their vertex in our high resolution tracking detectors based on capillary bundles filled with our LSs [9].

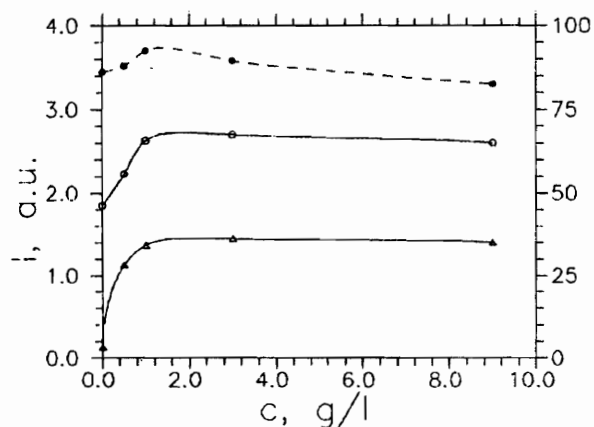


Fig. 9. Light output of 1MN + R6 versus the dopant concentration.  $\Delta$  – for  $T=20^{\circ}\text{C}$  in air;  $\circ$  – for  $T=-120^{\circ}$  in air;  $\bullet$  – for  $T=-120^{\circ}\text{C}$  in vacuum.

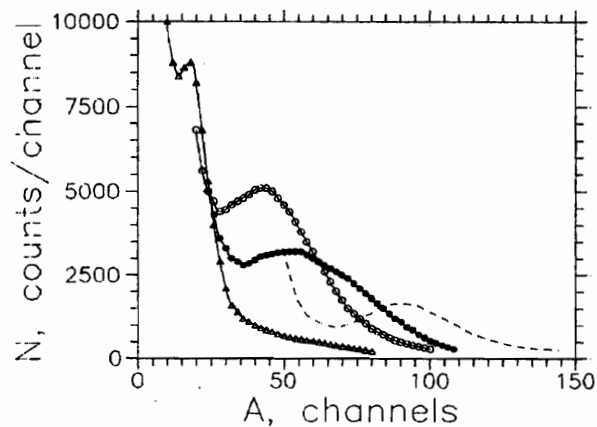


Fig. 10. Pulse height spectra of scintillation signals for  $\gamma$ -quanta of  $^{241}\text{Am}$  in 1MN + R45 (solid lines) and anthracene (dashed line).  $\Delta$  – at  $T=20^{\circ}\text{C}$  in air;  $\circ$  – at  $T=-120^{\circ}\text{C}$  in air;  $\bullet$  – at  $T=-120^{\circ}\text{C}$  in vacuum.

## 2.2. Thermal hysteresis of scintillators light output

As is clear from Figs. 3-6 all the tested scintillators, as well as pure solvents (Figs. 7-8), in the process of cooling down at certain temperatures, we observed fast transitions from low to high luminescent solid phases at  $T_{tr}^c$ . These transitions were always below their  $T_f$ . Only for scintillators based on 1MN (and pure 1MN) the temperature transitions were  $T_{tr}^c=-30^{\circ}\text{C}$ , which is very close to  $T_f=-28^{\circ}\text{C}$ . Figs. 3-4 also show that the scintillators



light outputs temperature transition in the process of heating up from higher luminescent phases to their ordinary levels occurs at  $T_{tr}^h = -11^\circ\text{C}$ , which does not coincide with their  $T_{tr}^c = -30^\circ\text{C}$ . In this case these light output temperature dependencies form loops of thermal hysteresis. One can see two loops of hysteresis for scintillators based on 1MN presented in Figs. 3-4 (and for pure 1MN solvent presented in Fig. 7) and only one loop — for scintillators based on other solvents presented in Figs. 5-6. The nature of these solid phases with different levels of luminescence in frozen scintillators and their pure solvents is not understood yet and needs explanation.

We investigated temporal properties of the observed thermal hysteresis. For this investigation 1MN + R6 was chosen, because it has two loops of hysteresis. In the process of the scintillator cooling down (Fig. 3) from  $T = 20^\circ\text{C}$ , we stabilized the temperature near  $T = -18^\circ\text{C}$ , i.e. at a low level of the light output  $I_{la} = 36.3\%$  in comparison with the anthracene. Within the accuracy of our measurements no changes of the light output were noticed during 40 min of observation. As expected, at this temperature the scintillator was in the liquid state. In the process of heating up the scintillator frozen at  $T = -120^\circ\text{C}$ , we also stabilized the temperature near  $T = -18^\circ\text{C}$ , i.e. at the upper level of the light output  $I_{sa} = 58.5\%$ . Within the accuracy of our measurements no changes of the light output were noticed during 40 min of observation. At the end of this period it was found that the scintillator remained in the solid state. Note that it took only about 1 min for our samples transition from liquid to solid states at their  $T_f$ .

The similar effect was also observed in the second loop of hysteresis, i.e. in solid state, at a low temperature  $T = -65^\circ\text{C}$  for 1MN + R6 (Fig. 3). In the process of cooling down in air to  $T = -65^\circ\text{C}$  the scintillator light output stabilized at a low level  $I_{sa} = 70\%$ . In the process of heating up the frozen scintillator to  $T = -65^\circ\text{C}$ , its light output stabilized at an upper level  $I_{sa} = 74.5\%$ . Within the accuracy of our measurements no changes of these light outputs were noticed during 40 min of observation. The nature of these effects needs explanation.

### 2.3. Decay times of frozen scintillators

The decay time constants  $\tau$  of the scintillator samples were measured by the single photoelectron delayed-coincidence counting technique [10] using FEU-71 PMs with quartz entrance windows. The scintillation in our samples was excited with a  $^{90}\text{Sr}$  radioactive  $\beta$ -source. The time resolution was about 0.5 ns and the accuracy of main decay time constants measurements was  $\pm 6\%$ . Our experimental setup did not allow us to measure decay time constants longer than 1000 ns and all the decay times of frozen scintillators in vacuum.

It is well known that the main part  $A_1^l \geq 96-97\%$  from the total light output of our promising LSs luminescence at  $T = 20^\circ\text{C}$  in air have short decay time constants of about  $\tau_1^l = 7.6-6.2$  ns [6] and the rest  $A_2^l \leq 3-4\%$  — have long decay time constants  $\tau_2^l = 40-25$  ns. The decay curves of our frozen in air scintillator samples were measured in a temperature interval from  $-120^\circ\text{C}$  to  $-50^\circ\text{C}$ . Some experimental results on the decay curve measurements for 1MN + R6 are presented in Fig. 11, where N are counts and t is the time.

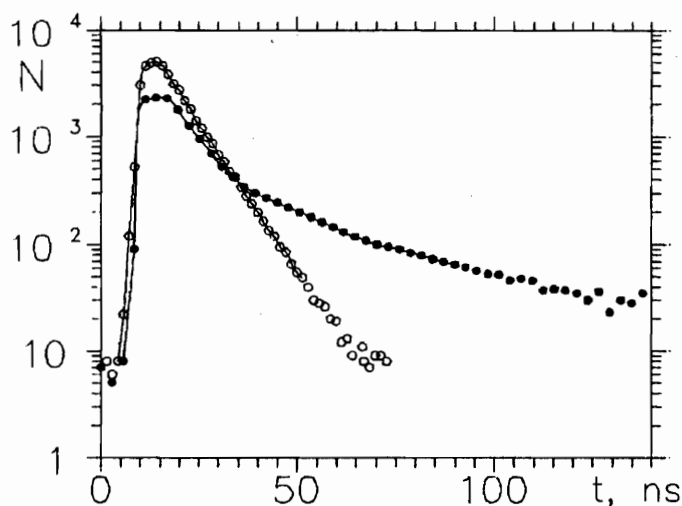


Fig. 11. Decay curves for 1MN + R6. o - for T=20°C in air; • - for T=-120°C in air.

The scintillator frozen in air showed that its first decay component became longer  $\tau_1^s=10.3$  ns than that at T=20°C  $\tau_1^l=7.6$  ns and less intensive. The second decay component with  $\tau_2^s=35$  ns remained practically unchanged, but significantly enhanced its intensity to a level of  $A_2^s=44$  % from the total light output. Possibly, a new and weak component with an intensity  $A_3^s=2$  % and a decay time constant  $\tau_3^s=1000$  ns appeared. Some experimental results on decay time constants measurements are summarized in Table 3.

Table 3. Decay time properties of liquid and frozen scintillators in air under high energy  $\beta$ -particles excitation.

N	Solvent	Dopant	$\tau_1^l$ , ns	$A_1^l$ , %	$\tau_2^l$ , ns	$A_2^l$ , %	$\tau_1^s$ , ns	$A_1^s$ , %	$\tau_2^s$ , ns	$A_2^s$ , %	$\tau_3^s$ , ns	$A_3^s$ , %
1	1MN	R6	7.6	96	40.	4	10.3	54	35.	44	1000.	2
2		R45	6.8	96	35.	4	11.3	58	32.	39	280.	3
3		R39	6.8	96	35.	4	7.7	71	29.	26	330.	3
4		3M-15	6.5	97	25.	3	7.5	75	25.	23	1000.	2
5	IPN	R6	6.3	96	40.	4	11.4	56	35.	41	1000.	3
6		R45	6.2	96	35.	4	11.2	56	35.	41	480.	3
7		R39	6.2	96	35.	4	6.8	77	31.	20	560.	3
8		3M-15	6.2	97	30.	3	8.4	76	29.	22	990.	2

One can see from Table 3 that all the frozen in air scintillators showed that their first decay components became longer, i.e.  $\tau_1^s=11.4-6.8$  ns, and less intensive than those at T=20°C in air. Their second decay components with  $\tau_2^s=40-25$  ns remained practically unchanged, but their intensities significantly enhanced to levels 20-44 % of the total light output. Possibly, a new and weak decay components with intensities  $\leq 2-3$  % and  $\tau_3^s=280-1000$  ns appeared.

## Conclusion

Frozen in vacuum at a temperature of about -120°C green emitting light scintillators based on 1-methylnaphthalene showed maximum light outputs up to 2.2-3.3 times higher relative to those levels in their liquid states at room temperature in air. Frozen in vacuum scintillator light outputs up to 92-144 % in comparison with the anthracene (taking into account the PM quantum efficiency) have been attained under high energy  $\beta$ -particle

excitation. These levels of frozen scintillators light outputs are 3.7-5.7 times higher in comparison with our standard polystyrene scintillator containing 1.5% + 0.01% POPOP having 1 cm thickness.

In the processes of cooling down to a temperature of about  $-120^{\circ}\text{C}$  and then heating up to  $20^{\circ}\text{C}$  in some temperature intervals all the tested scintillators revealed the thermal hysteresis effect of their light outputs.

All scintillators frozen in air showed that their first decay components became longer, i.e.  $\tau_1^f=11.4-6.8$  ns, and less intensive than those at room temperature in air. Their second decay components with  $\tau_2^f=40-25$  ns remained practically unchanged, but their intensities significantly enhanced to levels 20-44 % of the total light output. Possibly, a new and weak decay components with intensities  $\leq 2-3$  % and  $\tau_3^f=280-1000$  ns appeared.

The light outputs of our scintillators both in the liquid and solid states are sensitive to the density of ionization.

Frozen scintillators may find many applications especially in different types of particle detectors and calorimeters based on scintillators in high energy physics, for low energy particles detection in nuclear physics, etc.

### Acknowledgements

The authors would like to thank K.V.Zimyn for his help in scintillators light output measurements.

### References

- [1] S.V.Golovkin et al., Nucl. Instr. and Meth. A305 (1991) 385.
- [2] C.Cianfarani et al., Nucl. Instr. and Meth. A339 (1994) 449.
- [3] A.Cardini et al., Nucl. Instr. and Meth. A346 (1994) 163.
- [4] S.Buontempo, et al., Nucl. Instr. and Meth. A360 (1995) 7.
- [5] A.Cardini et al., Nucl. Instr. and Meth. A361 (1995) 129.
- [6] S.V.Golovkin et al., Preprint IHEP 96-13, Protvino, 1996.
- [7] S.V.Golovkin et al., Nucl. Instr. and Meth. A362 (1995) 283.
- [8] S.V.Golovkin et al., Preprint IHEP 97-12, Protvino, 1997.
- [9] P.Annis et al., Experimental results from large volume active target made of glass capillaries and liquid scintillator, Contribution to Wire Chambers Conference: Recent Trends and Alternative Techniques, Vienna, Austria, Feb.13-17, 1995.
- [10] L.M.Bolinger and G.E.Thomos Rev. Sci. Instr. 32 (1961) 1044.

*Received March 24, 1997*

## List of investigated solvents and dopants

1MN	- 1-methylnaphthalene, $T_f = -28^\circ\text{C}$
IPN	- naphthalene derivative, $T_f = -26^\circ\text{C}$
1PN	- 1-phenylnaphthalene $T_f = -7^\circ\text{C}$
pTP	- paraterphenyl, $\lambda_{em} = 340\text{ nm}$
POPOP	- 1,4-bis-(2-(5-phenyloxazolyl))- benzene, $\lambda_{em} = 420\text{ nm}$
R6	- pyrazoline derivative, $\lambda_{em} = 490\text{ nm}$
R39	- pyrazoline derivative, $\lambda_{em} = 485\text{ nm}$
R45	- pyrazoline derivative, $\lambda_{em} = 500\text{ nm}$
3M-15	- pyrazoline derivative, $\lambda_{em} = 500\text{ nm}$

Г.И.Бритвич и др.

Люминесцентные свойства замороженных сцинтилляторов.

Оригинал-макет подготовлен с помощью системы  $\text{IAT}_{\text{E}}\text{X}$ .

Редактор Е.Н.Горина.

Технический редактор Н.В.Орлова.

---

Подписано к печати 25.03.97. Формат 60 × 84/8.      Офсетная печать.

Печ.л. 1.25.    Уч.-изд.л. 0.96.    Тираж 240.    Заказ 985.    Индекс 3649.

ЛР №020498 17.04.97.

---

ГНЦ РФ Институт физики высоких энергий  
142284, Протвино Московской обл.

Индекс 3649

---

ПРЕПРИНТ 97-13,            ИФВЭ,            1997

---